International Journal of Current Research and Review
DOI: http://dx.doi.org/10.31782/IJCRR.2021.131306

Scopus

Original Research

IJCRR
Section: Healthcare
ISI Impact Factor (2019-20): 1.628
IC Value (2019): 90.81
SJIF (2020) = 7.893



# Performance Analysis of Flower Pollination Algorithm for Maximizing the Power Yield from Solar Photo-voltaic Arrays

**Hussain A[1], Khatri M[1*]**

[1]School of Electronics and Electrical Engineering, Lovely Professional University, Jalandhar -144411, Punjab, India.

## ABSTRACT

**Introduction:** In the energy crisis, the technologically equipped micro-grid is a boon to the electrical power generation system. Whereas the popular solar photo-voltaic (PV) micro-grids have self-sustained capabilities with minimum transmission line losses, no pollution, and power cuts. Moreover, yielding maximum power from the plant is a challenging task under different plant conditions and the use of an appropriate algorithm will support tracking the maximum PowerPoint.

**Aim and Methodology:** The objective is to yield the maximum power from the solar PV micro-grid. Therefore a more realistic three diode model of a solar photovoltaic cell is developed using basic equations to study the effectiveness of the proposed nature-inspired Flower Pollination Algorithm (FPA). The algorithm is applied to analyze the parameter variations of the model in comparison to Perturb and Observation (P&O), Ant Colony Optimization (ACO), Genetic Algorithm (GA), and Particle Swarm Optimization (PSO) algorithms to achieve the peak power. The simulations are performed on the Matlab version 2020a.

**Results and Conclusion:** The supremacy of the proposed method is judged from the power yield capability of the plant and significant improvement in fill factor from 0.75 to 0.81 has been observed with the proposed algorithm and the proposed algorithm achieved the maximum peak within 0.2 seconds compared to the other algorithms.

The variations in the nine parameters of the cell are analyzed with the proposed algorithm in comparison with the P&O, ACO, GA, and PSO proves the effectiveness of the proposed algorithm. The developed model trained using FPA for power peak tracking is verified for different shading patterns. The fill factor and power yield capacity of the micro-grid also improved along with the fast convergence.

**Key Words:** Flower pollination algorithm, Tracking power peak, Solar PV micro-grid, Three diode solar cell models, Maximum power generation

## INTRODUCTION

Renewable energy especially solar and wind are considered promising future generation systems. The power generated from such sources contributes to reform the environment along with technical and economic development. The solar PV micro-grids with properties such as irradiance presence in abundance, clean, maintenance, and noise-free is a support system to remote loads. It facilitates the electrical energy consumers with continuous and quality power.[1]The performance of solar panels plays a vital role in maximizing the power yield from such plants. Since the compiled solar panels of a plant are exposed to variable environmental conditions such as changes in solar irradiation pattern, partial shading condition, unexpected rain, etc.

Aforesaid conditions reduce the power conversion efficiency, increases the power frequency oscillations near the peak, reduces the chances to achieve global power peak and miserable failure in producing the energy to its capacity. There are several methods proposed by researchers to optimize the output power, one of them is to track the sun by positioning the solar panels and others are based on the application of different algorithms to reach out the maximum point in current-voltage (IV) and power-voltage(PV) characteristics curve.[2-3]

Although the PV panels are designed to generate maximum output power whereas the variations in irradiance, temperature, and load impedance affect the output current, voltage, and power respectively. Practically, the load line intersection

**Corresponding Author:**
**Khatri Megha,** School of Electronics and Electrical Engineering, Lovely Professional University, Jalandhar -144411, Punjab, India.
E-mail: megha.25035@lpu.co.in

**ISSN:** 2231-2196 (Print) **ISSN:** 0975-5241 (Online)

**Received:** 14.11.2020 **Revised:** 10.01.2021 **Accepted:** 17.03.2021 **Published:** 05.07.2021

on the IV curve is far away from the peak power point in case of direct connection of load with the panels, which is required to be adjusted under unstable conditions to obtain the maximum output. Therefore converters are inserted between the solar panels and charge-controlled storage batteries/loads.[4]

The direct current to direct current (DC/DC) converter is placed when the panels are serving DC loads and a direct current to Alternative current (DC/AC) converter is installed for AC loads. To reach the maximum power peak the duty cycle of the converters is essential to be controlled. In other words, the converters act as a mediator in source to load impedance matching.[5-7]Moreover the overall efficiency of the solar PV micro-grid relies upon the efficiency of PV panels, battery charge controllers, converters, and computational method. The computational methods may differ in convergence speed, complexity, sensors required, cost, hardware implementation, etc. With the application of any of the computational algorithms, the global optimum peak can be achieved at different time durations.[5-6]

In this work, the focus is on Flower Pollination Algorithm (FPA) as shown in figure1; because of independence on initial population and an extended ability to explore as well as exploit the search space.[6] Thus require lesser efforts to regulate the parameters. The remaining part of the paper is organized as follows. Section 2 explains the modelling of the solar PV cell, section 3 describes the control structure of the proposed methodology with detailed steps on FPA implementation. In section 4 comparison of the proposed algorithm with Perturb and observation (P&0-Hill climbing)[7-8], Genetic Algorithm (GA)[9], Particle swarm optimization (PSO)[10], Ant Colony Optimization (ACO)[11], and simulation studies with different shading patterns of FPA trained micro-grid is discussed.[6-12] Also the power yield capacity of the proposed algorithm is compared. Finally, conclusions derived are presented at the end.

**Figure1** illustrates the continuous monitoring of current ($I_{PV}$) and voltage ($V_{PV}$) generated by the solar arrays and with the help of FPA the array parameters are compared with the reference and the difference in parameters helps in updating the duty cycle, which in response generate the pulses for DC/DC boost converter to extract the maximum power output and reducing the gap between actual and expected IV curve.

## Mathematical Model

A three diode equivalent model is mathematically expressed instead of single and double diode models. In the case of low irradiance; the single diode model is deficient in precision in open-circuit voltage, therefore, carries recombination losses in the depletion region and the double diode model has reduced recombination losses but shows better accuracy in this case but lacks in addressing the leakage currents.[13] Therefore a more precise three diode model is considered for the thorough examination of the associated parameters which steers the power yield.

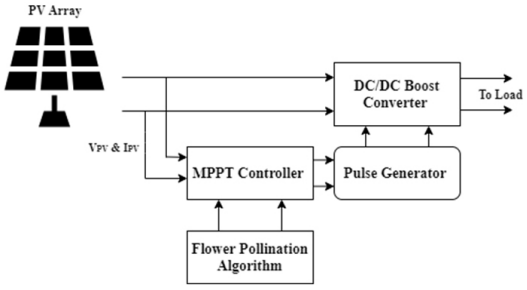


**Figure 1:** Block Diagram of Flower Pollination Algorithm.

**Figure 2** presents the three diode model of solar cells to exhort the maximum power from solar irradiance (G kW/m$^2$) at reference temperature ($T_{ref}$). This generates the photocurrent flowing through the layers of solar cells represented as diodes. Initially, the series resistance $R_S$ is kept lower compared to the shunt resistance $R_{SH}$ that is further modified using proffered algorithm to deliver maximum current to the load. The mathematical equations involved are consisting of photocurrent $I_p$, photocurrent at referred temperature $I_{p(Tref)}$, and constant (K) presented in equation (1).

$$I_p = I_{p(T_{ref})} * (1 + K(T - T_{ref})) \quad (1)$$

Where the photocurrent at reference temperature 25$^0$C depends upon the ratio of the level of irradiance $G_T$ at cell temperature T with irradiance $G_{(Tref)}$ at reference temperature i.e. 1000W/m$^2$( Equation 2).

$$I_{p(T_{ref})} = \frac{G_T}{G_{(Tref)}} * I_{SC(ref)} \quad (2)$$

And constant (K) is reliant on the short circuit current $I_{SC}$, expressed in equation 3.

$$K = \frac{I_{SC(T)} - I_{SC(T_{ref})}}{T - T_{ref}} \quad (3)$$

To better illustrate the experimental data, a model with three diodes has been suggested in **Fig 2**.

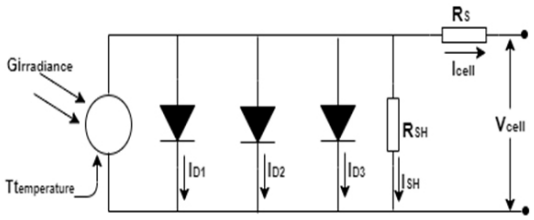


**Figure 2:** Three diode model of solar cell.

The diode currents $I_{D1}$, $I_{D2}$, $I_{D3}$ in equation (4), (5) and (6) varies with reverse saturation currents $I_{o1}$, $I_{o2}$, $I_{o3}$. Where $V_{T1}$, $V_{T2}$, $V_{T3}$ are the thermal voltages and $\alpha_1$, $\alpha_2$, $\alpha_3$ represent the ideality factor of diodes $D_1$, $D_2$, $D_3$ respectively presented in equation 4-8.

$$I_{D1} = I_{o1}\left[exp\left(\frac{V_{cell}+I_{cell}*R_S}{\alpha_1 V_T}\right)-1\right] \quad (4)$$

$$I_{D2} = I_{o2}\left[exp\left(\frac{V_{cell}+I_{cell}*R_S}{\alpha_2 V_T}\right)-1\right] \quad (5)$$

$$I_{D3} = I_{o3}\left[exp\left(\frac{V_{cell}+I_{cell}*R_S}{\alpha_3 V_T}\right)-1\right] \quad (6)$$

Further, the reverse saturation currents can be calculated as:

$$I_{o1,2,3} = I_{o,ref}\left(\frac{T_{ref}}{T}\right)^3 e^{\frac{qE_g}{\alpha k}\left(\frac{1}{T_{ref}}-\frac{1}{T}\right)} \quad (7)$$

and

$$E_g = E_{g,ref}(1-0.00026(T-T_{ref})) \quad (8)$$

Where $E_{g,ref}$= 1.121eV for silicon cells.[12]

The parallel and series resistance values can be obtained by iterations and here the mathematical expression for calculating $R_{SH}$ is presented in equation (9). With excessively high values of series, resistance $R_S$ the short circuit current decreases and thus impacts the fill factor. The low valued shunt resistance $R_{SH}$ may cause significant power losses by providing an alternating path to the generated photocurrent $I_p$ and affects the fill factor shown in equation 10 and 11. Therefore both the resistances are considered as variable parameters where the series resistance depends on the connected load.

$$R_{SH} = \frac{V_{mp}(V_{mp}+I_{mp}R_S)}{(V_{mp}(I_p-I_{D1}-I_{D2}-I_{D3})-P_{mp})} \quad (9)$$

and the current $I_{SH}$ in the shunt branch of the model is given below

$$I_{SH} = \frac{V_{cell}+I_{cell}*R_S}{R_{SH}} \quad (10)$$

The cell current ($I_{t'll}$) can be mathematically expressed using the presented equation

$$I_{cell} = I_p - I_{D1} - I_{D2} - I_{D3} - \frac{V_{cell}+I_{cell}*R_S}{R_{SH}} \quad (11)$$

The power (P) acquired from the single photovoltaic module is given in equation (12),

Where $N_S$ = number of photovoltaic cells in series and

$N_p$ = number of photovoltaic cells in parallel.

$$P = (N_S*N_P)\,V_{cell}*I_{cell} \quad (12)$$

Calculated peak voltage ($V_{mp}$) and peak current ($I_{mp}$) in equation (13-16)

$$V_{mp} = V_{mp,ref}\left[1+0.0539log\left(\frac{G_T}{G_{T,ref}}\right)+\beta\,\Delta T\right] \quad (13)$$

where β is the voltage temperature coefficient (in volt per℃).

$$I_{mp} = I_{SC,ref}\left[1-K_1\left\{exp\left(\frac{V_{mp}-\Delta V}{K_2 V_{OC,ref}}\right)-1\right\}\right]+\Delta I \quad (14)$$

$$\text{With } K_1 = \left(1-\frac{I_{mp,ref}}{I_{SC,ref}}\right)exp\left(-\frac{V_{mp,ref}}{K_2*V_{OC,ref}}\right) \quad (15)$$

$$\text{And } K_2 = \frac{\left(\frac{V_{mp,ref}}{V_{OC,ref}}-1\right)}{ln\left(1-\frac{I_{mp,ref}}{I_{SC}}\right)} \quad (16)$$

Hence the maximum power ($P_{mp}$) = $V_{mp}$*$I_{mp}$ also the fill factor of the PV curve expressed in equation 17:

$$FF = \frac{V_{mp}*I_{mp}}{V_{OC}*I_{SC}} \quad (17)$$

And the maximum FF can be calculated theoretically using equation (18), in other words, the power peak in P-V characteristics of the panel can be obtained.

$$\frac{dP}{dV} = \frac{d(VI)}{dV} = I\frac{dV}{dV}+V\frac{dI}{dV} = I_{mp}+V_{mp}\frac{d\,I_{mp}}{d\,V_{mp}} = 0 \quad (18)$$

The panel voltage $V_{PV}$ is the summation of voltages across each cell connected in series of the panel and current $I_{PV}$ remains equal to the current produced by an individual cell. The performance of the complete system depends upon the nine parameters $\delta = I_p, I_{o1}I_{o2}I_{o3}, \alpha_1, \alpha_2, \alpha_3, R_S, R_{SH}$ which are variable concerning changes in internal and external factors such as environment, load, etc shown in equation 19.

$$RMSE = \sqrt{\frac{1}{n}\sum_{i=1}^{n} f_i^2(V,I,\delta)} \quad (19)$$

Thus defines the objective function f(V, I,$\delta$) for the optimal values. The target achievement can be judged by reducing the root mean square error (RMSE) between the reference and currently observed values which also depicts the fitness of solutions.

## Proposed Approach

Bio-inspired Flower pollination algorithm and its variants are applicable in solving the optimization related problems in the field of engineering introduced by Yang .[14] Extension from the single objective problems to the multi-objective

optimization problems were purposed by Yang, & Karamanoglu.[15] Pollination is an observable fact refers to the transmit of pollens from one to another flower using their species or other species for reproduction.

The transfer of pollens through pollinators in the flowers of the same plants is called self-pollination and to different plants known as cross-pollination. The birds, insects, animals are known as biotic pollinators and the abiotic pollinator are wind, water, etc. Cross-pollination through the biotic process is the most common and considered global pollination. On the other hand, self-pollination through the abiotic process is viewed as local pollination. The switching probability P∈ [0,1] limits the self and cross-pollination and the flower consistency depends upon the flowers involved. As global pollinators, the birds can fly long distances and shows Lévy flight behaviour.[16]

Using Lévy distribution the global pollination is mathematically generalized given equation 20.

$$X_i(t+1) = X_i(t) + \gamma L(\rho)(G_* - X_i^t(t)) \quad (20)$$

Where $X_i^t$ i = 1, 2, 3,....n is i[th] pollen or solution vector $X_i$ at iteration t, $G_*$ is the current best solution(duty cycle) established in the current population, γ is scaling factor which alters the step size and L($\rho$) is the step size extracted from Lévy distribution equation(21) i.e. the flight of pollens (**Figure 3**).

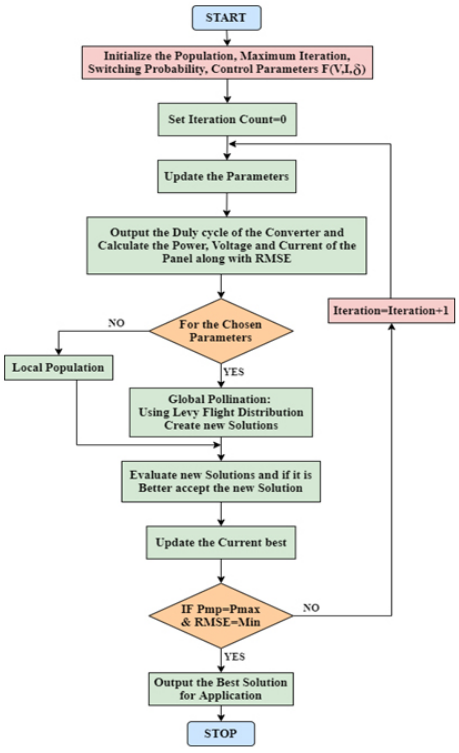


**Figure 3:** Flow chart of proposed flower pollination algorithm.

$$L \sim \frac{\rho\tau(\rho)\sin(\pi\rho/2)}{\pi}\frac{1}{s^{1+\rho}} \quad (21)$$

Where $\tau(\rho)$ is the standard gamma function and this allotment is applicable for large steps S>0. If the chosen random number does not fit with the switching probability limits, the local pollination takes place presented in equation 22.

$$X_i(t+1) = X_i(t) + \varepsilon\left(X_j^t(t) - X_k^t(t)\right) \quad (22)$$

Where $X_j^t$ and $X_k^t$ are pollen from diverse flowers of similar plant species, which signify flower consistency for local pollination and the local distribution $\varepsilon \in [0,1]$ It is very much advantageous to validate this method because it explores globally and exploits locally for finding the optimum solution.

**Figure 3** is a flow chart of the proposed algorithm where the initial population i.e. set of random solutions are taken along with generated voltage and current from the solar arrays, nine control parameters i.e. $\delta = I_p, I_{o1}I_{o2}I_{o3}, \alpha_1, \alpha_2, \alpha_3, R_S, R_{SH}$ , switching probability and initial iteration count=0. To reduce the root-mean-square-error between the reference and actual parameters, also to modify the duty cycle to yield the maximum output. The levy's distribution helps in identifying the global best solution to extract peak power. When the obtained power is equal to the reference with the secured parameters the process will be terminated. The algorithm brings randomness with each iteration through self-pollination, which further reduces the number of iterations, implementation steps, and complexity of computation to achieve the optimum values.

## RESULTS AND DISCUSSIONS

The performance of the chosen algorithm is evaluated at different shading patterns of the solar PV panels connected to a virtual micro-grid of 40 (10 parallel strings with 4 series joined modules per string) modules and the power production capacity of 9to12KW and each module with specifications in table1. The simulation model of the algorithm for following the global maximum of power peak is in **figure 4**: which shows the simulation blocks with the proffer algorithm with maximum power point tracking controller which is regulating the voltage and current to improve upon the IV curve of the solar arrays and fill factor (**Table 1**). The regulated current output is further compared with the reference signals to update the duty cycle. The performance of the algorithm is also studied with different shading patterns.

**Figure 5** is the actual photographs of the devices named pyrometer is used as irradiance sensor, the photovoltaic modules connected in series and parallel, the module string

connector box, and the maximum power point tracking controlled inverter. The DC/DC boost converter with controllable frequency is 10 kHz, the capacitance of 150 μF and inductance of 20 mH is used. The performance of the proposed algorithm depends upon the duty cycle of the converter which is initially obtained on random selection bases with a sampling time of 0.02seconds.

The effectiveness of the algorithm in comparison to other techniques is presented in **table 2**. Using the proposed algorithm maximum voltage and current can be obtained from the cell with minimum series resistance 0.2682Ω.

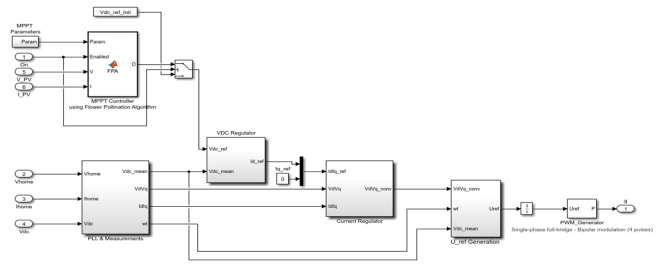

**Figure 4:** Simulation blocks with the proposed algorithm.

**Figure 5:** (a) Pyranometer (b) Photovoltaic Modules (c) String connectors (d) Inverter.

**Table 1: Specifications of Solar Photo-voltaic Panel**

| Parameters | Lifeline Energy International LLE-6M305 |
|---|---|
| Number of cells in series per module | 72 |
| Maximum Power($P_{max}$) | 300.352 W |
| Maximum Voltage($V_{mp}$) | 36.1V |
| Maximum Current($I_{mp}$) | 8.32A |
| Short Circuit Current($I_{SC}$) | 8.77A |
| Open Circuit Voltage($V_{OC}$) | 45.4V |
| $I_{SC}$ temperature coefficient (A/ °C) | 0.083295 |
| $V_{OC}$ temperature coefficient of (V/ °C) | -0.41271 |

However, a significant improvement in fill factor from 0.75 to 0.81 has been observed with the proposed algorithm. The disparity in other parameters can also be noticed. In figure 6 the power yield from the modules is shown and the proposed algorithm achieved the maximum peak within 0.2 seconds of time compared to the other algorithms. **Table3** illustrates the capability of the proposed algorithm in maintaining the voltage and current under different shading patterns of the modules and it can be observed despite the shading the algorithm maintained the power peak (Figure 6).

**Table 2: Parameter Variations of Proposed Algorithm**

| Cell Parameters | Perturb and Observation (P&O-Hill Climbing) | Ant Colony Optimization (ACO) | Genetic Algorithm (GA) | Particle Swarm Optimization (PSO) | Flower Pollination Algorithm (FPA) |
|---|---|---|---|---|---|
| $I_p$ | 8.7629 | 8.7954 | 8.7041 | 8.8158 | 8.8551 |
| $I_{01}$ | $2.946x10^{-8}$ | $0.918x10^{-8}$ | $2.691x10^{-8}$ | $1.413x10^{-8}$ | $1.896x10^{-8}$ |
| $I_{02}$ | $2.691x10^{-9}$ | $4.145x10^{-9}$ | $1.691x10^{-9}$ | $3.804x10^{-9}$ | $1.632x10^{-9}$ |
| $I_{03}$ | $4.353x10^{-9}$ | $1.693x10^{-9}$ | $3.770x10^{-9}$ | $4.495x10^{-9}$ | $1.695x10^{-9}$ |
| $\alpha_1$ | 1.4109 | 1.1616 | 1.095 | 1.0554 | 1.2192 |
| $\alpha_2$ | 1.2042 | 1.0231 | 1.2313 | 1.1864 | 1.1468 |
| $\alpha_3$ | 1.0139 | 1.4428 | 1.175 | 1.4801 | 1.1907 |
| $R_S$ | 0.4660 | 0.4056 | 0.4194 | 0.3987 | 0.2682 |
| $R_{SH}$ | 1157.0391 | 1182.114 | 1097.003 | 900.445 | 1196.204 |

**Table 3: Performance of FPA under different shading patterns**

| Shading patterns (Number of shaded cells in each module) | No Shading | Pattern:1 4series modules shaded | Pattern:2 8 series modules shaded | Pattern:3 12series modules shaded | Pattern:4 16series modules shaded | Pattern:5 20 series modules shaded |
|---|---|---|---|---|---|---|
| Average Arrays Temperature ( °C) | 38.80 | 38.48 | 38.10 | 37.63 | 37.07 | 36.94 |
| Module Maximum Voltage $V_{mp}$ (V) | 35.60 | 35.51 | 35.40 | 35.39 | 35.30 | 35.12 |
| Module Maximum Current $I_{mp}$(A) | 8.26 | 8.21 | 8.19 | 7.98 | 7.97 | 7.90 |
| Array Maximum Power $P_{mp}$($kW_h$) | 11.76 | 10.49 | 9.27 | 7.90 | 6.75 | 5.57 |

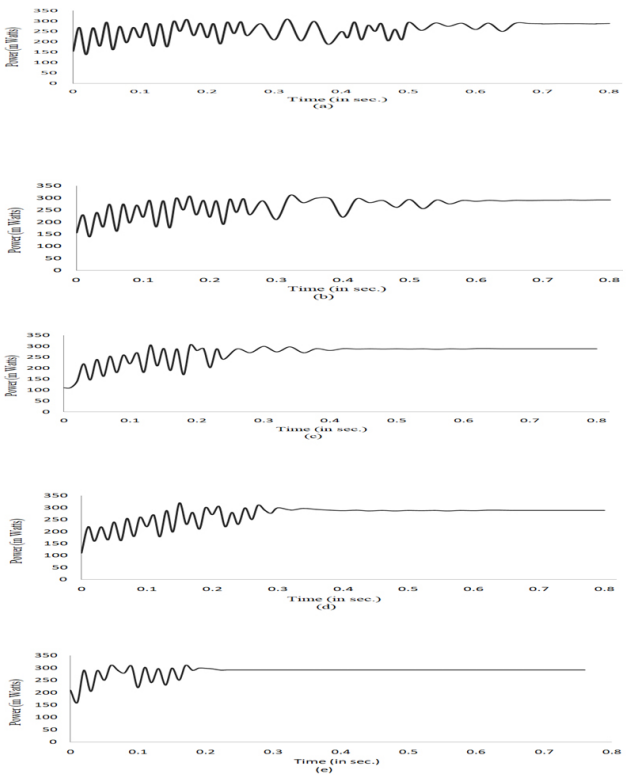


**Figure 6:** Power yield with Different Algorithms (a) P&O (b) ACO (c) GA (d) PSO (e) FPA.

## CONCLUSIONS

A three diode model of the solar photovoltaic cell is developed using basic equations to study the effectiveness of nature-inspired flower pollination algorithm for power yield. The variations in the nine parameters of the cell are analyzed with the proposed algorithm in comparison with the perturb and Observation(P&O), Ant Colony Optimization (ACO), Genetic Algorithm(GA), and Particle Swarm Optimization (PSO) proves the effectiveness of the proposed algorithm. The fill factor and power yield capacity of the micro-grid also improved along with the fast convergence. The developed model trained using Flower Pollination Algorithm(FPA)for power peak tracking is verified for different shading patterns. Thus it is proven that the proposed algorithm is best suited for yielding maximum power with an exceptional power peak tracking record.

## ACKNOWLEDGEMENTS

I take this opportunity to express profound gratitude and deep regards to whom I cited their papers and I am also grateful to Lovely Professional University for providing me with an adequate infrastructure and facilities to carry out the investigation.

**Conflict of interest-** The authors declare that there is no conflict of interest associated with this publication.

**Funding-** none

**Author's contribution-** Conceptualization, Methodology, Mathematical analysis, and Simulation, Article Drafting[1]

Acquisition of Data, Analysis, and Interpretation of Data, Article Review, Supervision and Guidance[2]

## REFERENCES

1. Ishaque K, Salam Z. A review of maximum power point tracking techniques of PV system for uniform insolation and partial shading condition. Renew Sustain Energy Rev. [Internet]. 2013;19:475–88. Available from: http://dx.doi.org/10.1016/j.rser.2012.11.032
2. Draa A. On the performances of the flower pollination algorithm - Qualitative and quantitative analyses. Appl Soft Comput J. [Internet]. 2015;34:349–71. Available from: http://dx.doi.org/10.1016/j.asoc.2015.05.015
3. Meyer EL. Extraction of Saturation Current and Ideality Factor from Measuring Voc and Isc of Photovoltaic Modules. Int J Photoenergy. 2017;2017.
4. Koutroulis E, Blaabjerg F. A new technique for tracking the global maximum power point of PV arrays operating under partial-shading conditions. IEEE J Photovoltaics. 2012;2(2):184–90.

5. Qais MH, Hasanien HM, Alghuwainem S. Identification of electrical parameters for three-diode photovoltaic model using analytical and sunflower optimization algorithm. Appl Energy [Internet]. 2019;250(April):109–17. Available from: https://doi.org/10.1016/j.apenergy.2019.05.013
6. Abdelsalam AK, Massoud AM, Ahmed S, Enjeti PN. High-performance adaptive Perturb and observe MPPT technique for photovoltaic-based microgrids. IEEE Trans Power Electron. 2011;26(4):1010–21.
7. Khatri M, Kumar A. Simulation and experimental validation of a hill-climbing algorithm for maximum power point tracking of a solar photovoltaic plant. Curr Sci. 2017;113(7):1423–8.
8. Khatri M. Simulation and Experimental Fault Analysis of Grid Tied Solar Photo-Voltaic System. SSRN Electron J. 2018; 27(7): 381-385.
9. Borni A, Bouarroudj N, Bouchakour A, Zaghba L. P&O-PI and fuzzy-PI MPPT Controllers and their time-domain optimization using PSO and GA for the grid-connected photovoltaic system: a comparative study. Int J Power Electron. 2017;8(4):300.
10. Cheng Z, Zhou H, Yang H. Research on MPPT control of PV system based on PSO algorithm. 2010 Chinese Control Decis Conf CCDC 2010. 2010;887–92.
11. Priyadarshi N, Ramachandaramurthy VK, Padmanaban S, Azam F. An ant colony optimized mppt for standalone hybrid PV-wind power system with single cuk converter. Energies. 2019;12(1): 47-51.
12. Selem SI, El-Fergany AA, Hasanien HM. Artificial electric field algorithm to extract nine parameters of the triple-diode photovoltaic model. Int J Energy Res. 2021;45(1):590–604.
13. El-Hameed MA, Elkholy MM, El-Fergany AA. Three-diode model for characterization of industrial solar generating units using Manta-rays foraging optimizer: Analysis and validations. Energy Convers Manag [Internet]. 2020;219(March):113048. Available from: https://doi.org/10.1016/j.enconman.2020.113048
14. de Alcântara Neto MC, Ferreira HRO, de Araújo JPL, Barros FJB, Neto AG, de Oliveira Alencar M, et al. Compact ultra-wideband FSS optimised through fast and accurate hybrid bio-inspired multiobjective technique. IET Microwaves, Antennas Propag. 2020;14(9):884–90.
15. Yang X-S, Karamanoglu M. Nature-inspired computation and swarm intelligence: a state-of-the-art overview [Internet]. Nature-Inspired Computat Swarm Intelligence. Elsevier Ltd; 2020. 3–18. Available from: https://doi.org/10.1016/B978-0-12-819714-1.00010-5
16. Ghezal F, Belal T, Tala-Ighil Zair R. Fabrication and characterization of cuinse2 thin-film solar cells with fluorine-doped zno as new buffer layer. Chalcogenide Lett. 2020;17(10):521–7.